Regulatory Toxicology and Pharmacology 81 (2016) S82–S92

Contents lists available at ScienceDirect

Regulatory Toxicology and Pharmacology

journal homepage: www.elsevier.com/locate/yrtph

Evaluation of the Tobacco Heating System 2.2 (THS2.2). Part 5: microRNA expression from a 90-day rat inhalation study indicates that exposure to THS2.2 aerosol causes reduced effects on lung tissue compared with cigarette smoke

Alain Sewer [a, *], Ulrike Kogel [a], Marja Talikka [a], Ee Tsin Wong [b], Florian Martin [a], Yang Xiang [a], Emmanuel Guedj [a], Nikolai V. Ivanov [a], Julia Hoeng [a], Manuel C. Peitsch [a]

[a] Philip Morris International R&D, Part of Philip Morris International Group of Companies, Philip Morris Products S.A., Quai Jeanrenaud 5, 2000, Neuchâtel, Switzerland

[b] Philip Morris International Research Laboratories Pte Ltd, Part of Philip Morris International Group of Companies, 50 Science Park Road, The Kendall #02-07, Science Park II, 117406, Singapore

ARTICLE INFO

Article history:
Received 4 July 2016
Received in revised form
7 November 2016
Accepted 16 November 2016
Available online 17 November 2016

Keywords:
Heat-not-burn
Modified risk tobacco product
Inhalation toxicology study
microRNA expression
Inflammation-related microRNAs

ABSTRACT

Modified-risk tobacco products (MRTP) are designed to reduce the individual risk of tobacco-related disease as well as population harm compared to smoking cigarettes. Experimental proof of their benefit needs to be provided at multiple levels in research fields. Here, we examined microRNA (miRNA) levels in the lungs of rats exposed to a candidate modified-risk tobacco product, the Tobacco Heating System 2.2 (THS2.2) in a 90-day OECD TG-413 inhalation study. Our aim was to assess the miRNA response to THS2.2 aerosol compared with the response to combustible cigarettes (CC) smoke from the reference cigarette 3R4F. CC smoke exposure, but not THS2.2 aerosol exposure, caused global miRNA downregulation, which may be explained by the interference of CC smoke constituents with the miRNA processing machinery. Upregulation of specific miRNA species, such as miR-146a/b and miR-182, indicated that they are causal elements in the inflammatory response in CC-exposed lungs, but they were reduced after THS2.2 aerosol exposure. Transforming transcriptomic data into protein activity based on corresponding downstream gene expression, we identified potential mechanisms for miR-146a/b and miR-182 that were activated by CC smoke but not by THS2.2 aerosol and possibly involved in the regulation of those miRNAs. The inclusion of miRNA profiling in systems toxicology approaches increases the mechanistic understanding of the complex exposure responses.

1. Introduction

The U.S. Family Smoking Prevention and Tobacco Control Act (FSPTCA) defines a MRTP as "any tobacco product that is sold or distributed for use to reduce harm or the risk of tobacco related disease associated with commercially marketed tobacco products" (Family Smoking Prevention and Tobacco Control Act). This publication is part of a series of nine publications describing the nonclinical and part of the clinical assessment of a candidate MRTP, THS2.2, and a mentholated version (THS2.2M). The series of publications provides part of the overall scientific program to assess the potential for THS2.2 to be a reduced-risk product. The first publication in this series describes THS2.2 and the assessment program for MRTPs (Smith et al., 2016). This is followed by six publications, including this one, that describe the nonclinical assessment of THS2.2 regular and THS2.2M (Kogel et al., 2016; Oviedo et al., 2016; Schaller et al., submitted (this issue)-a; Schaller et al., submitted (this issue)-b; Sewer et al., 2016; Wong et al., 2016). The eighth publication in the series describes a clinical study to assess whether the reduced formation of Harmful and Potentially Harmful Constituents (HPHC) for THS2.2 regular also leads to reduced-exposure to HPHCs when the product is used in a clinical setting (Haziza, 2016). A final publication utilizes data gathered from the reduced exposure clinical study on THS2.2 regular to determine if a systems pharmacology approach can identify exposure response markers in

* Corresponding author.
E-mail address: alain.sewer@pmi.com (A. Sewer).

http://dx.doi.org/10.1016/j.yrtph.2016.11.018

Abbreviations

CC	Combustible Cigarette
CS	Cigarette Smoke
FDR	False Discovery Rate
GC	Guanine-Cytosine
HPHC	Harmful and Potentially Harmful Constituents
IL-1	Interleukin 1
lncRNA	Long Non-Coding RNA
mRNA	Messenger RNA
miRNA	MicroRNA
MRTP	Modified Risk Tobacco Product
NPA	Network Perturbation Amplitude
NUSE	Normalized Unscaled Standard Error
OECD	Organisation for Economic Co-operation and Development
QC	Quality Control
Q-Q	Quantile-Quantile
RT-PCR	Reverse Transcription Polymerase Chain Reaction
TG	Test Guidelines
THS2.2	Tobacco Heating System 2.2
TNF	Tumor Necrosis Factor

peripheral blood of smokers switching to THS2.2 (Martin et al., 2016).

In this article, the expression of microRNA (miRNA) molecules in the lungs of rats exposed to the novel Tobacco Heating System (THS) 2.2 product in a 90-day OECD TG-413 inhalation study are investigated. One goal is to integrate the findings obtained from the analyses of miRNA exposure responses into the systems toxicology framework applied to the same study and reported earlier in this publication series (Wong et al., 2016).

miRNAs are noncoding regulatory RNA molecules that bind target messenger RNAs (mRNAs) and destabilize them or suppress their translation into proteins (Krol et al., 2010). There is increasing evidence that miRNA levels are affected by several known toxicants as well as oxidative and other forms of cellular stress. This suggests an important role for miRNAs in toxicology, which could provide a link between environmental influences and gene expression (Hong and Cho, 2015). Different types of cellular stress have been shown to affect genes encoding miRNAs as a mechanism of adaptation or tolerance to stress factors (Lema and Cunningham, 2010). In fact, multiple stressors including reactive oxygen species, phorbol esters, the RAS oncogene, double-stranded RNA, and interferons can affect the levels of the RNase III enzyme Dicer, which is critical for the generation of miRNAs (Wiesen and Tomasi, 2009).

miRNAs have also been linked to diseases etiologically related to smoking, such as lung cancer (Liu et al., 2009) and chronic obstructive pulmonary disease (De Smet et al., 2015). An alteration of the miRNA profile induced by CC smoke was found in target tissues even before disease manifestation, as recently reviewed (Vrijens et al., 2015). Izzotti et al. (2009a) showed that exposure to environmental CC smoke for 4 weeks resulted in downregulation of several miRNAs in rat lungs. Similar studies in mice showed that, in addition to sex and age, environmental CC smoke exposure for 5 weeks induced changes in the pulmonary miRNA profile. Mostly downregulated, the affected miRNAs were involved in adaptive mechanisms and the activation of pathways known to be associated with lung diseases (Izzotti et al., 2009b). Moreover, miRNA profiling of human bronchial brushings identified several miRNAs that were downregulated in smokers compared with those in nonsmokers and further *in vitro* tests showed that miR-218 in particular was suppressed by CC smoke condensate in cultured primary bronchial epithelial cells (Schembri et al., 2009). In organotypic bronchial epithelial cultures exposed to fresh cigarette smoke (CS) at the air–liquid interface, we previously observed reduced miR-146a/b levels related to inflammatory gene expression changes, and reduced levels of miR-449a/b/c and miR-107 related to changes in the expression of genes regulating the cell cycle (Mathis et al., 2013). In addition, different CC smoke-related miRNA response profiles were observed in lung tumors and tumor-free lung parenchyma samples from A/J mice exposed to CC smoke for 18 months when compared with spontaneous lung tumors and parenchyma from sham-exposed mice (Luettich et al., 2014).

The overall study was designed and conducted in accordance with the OECD TG-413 guidelines and the results are summarized in an accompanying manuscript (Wong et al., 2016). Briefly, rats exposed to mainstream CC smoke from 3R4F reference cigarettes for 90 days showed inflammation as indicated by the accumulation of immune cells in the lung tissue as well as proinflammatory and chemotactic cytokines in bronchoalveolar lavage fluid. Histopathological findings in the respiratory tract included epithelial cell hyperplasia, squamous metaplasia, atrophy in the airways, and the accumulation of pigmented alveolar macrophages in the lungs of 3R4F-exposed rats. All of these effects were markedly reduced in rats exposed to the aerosol from THS2.2. Here, we report on the pulmonary miRNA expression after 90-day inhalation of THS2.2 in comparison with 3R4F, as well as after a 42-day postexposure recovery period. The miRNA findings in the lung tissue of rats exposed to CC smoke or THS2.2 aerosol were complemented by transcriptomic profiling to obtain an insight into the mechanism behind the observed effects.

2. Materials and methods

2.1. Experimental design

Here, we report on the "OECD plus" part of a 90-day rat inhalation study in accordance with OECD test guidelines (TG) 413 (Wong et al., 2016). Experimental groups consisted of six male and six female rats. 'Exposed' experimental groups were scheduled for 13 weeks or 90 days (90d) of exposure for 5 days per week and 6 hours per day to *sham* (filtered air), *3R4F low* (8 μg/l nicotine), *3R4F medium* (15 μg/l nicotine), *3R4F high* (23 μg/l nicotine), *THS2.2 low* (15 μg/l nicotine), *THS2.2 medium* (23 μg/l nicotine), or *THS2.2 high* (50 μg/l nicotine) treatments, in accordance with OECD TG. 'Recovery' experimental groups consisted of rats concomitantly exposed with the 90-day animals, which were kept for additional 42 days of post-exposure recovery (90 + 42d). The *THS2.2 high* treatment was not included in the recovery groups because of the exposure chamber capacity. Here, we specifically report on the miRNA analysis of the lung after the inhalation and recovery period. After sample prioritization, all male rat exposed and recovery groups could be used for miRNA profiling, whereas the female rat *3R4F low* and *3R4F medium* groups (90d and 90 + 42d) were not available.

2.2. Animals

All procedures involving animals were performed in an American Association for the Accreditation of Laboratory Animal Care-accredited, Agri-Food & Veterinary Authority of Singapore-licensed facility with approval from an Institutional Animal Care and Use Committee, and performed in compliance with guidelines set by the National Advisory Committee for Laboratory Animal Research (NACLAR, 2004).

Outbred male and female Sprague–Dawley rats [Crl: CD (SD)], bred under specific pathogen-free conditions, were obtained from Charles River (Wilmington, MA, USA). The rats were approximately 8 weeks old at arrival and were acclimatized for at least 14 days prior to exposure.

2.3. Reference cigarettes and THS2.2 tobacco sticks

Reference 3R4F cigarettes were purchased from the University of Kentucky (Lexington, KY, USA; http://www.ca.uky.edu/refcig). THS2.2 *tobacco sticks* were provided by Philip Morris Products S.A. (Neuchâtel, Switzerland). THS2.2 sticks consist of a tobacco plug made of specially processed tobacco powder, a transfer section, and a mouthpiece, wrapped with cigarette paper. These sticks are designed to be inserted into a stick holder that includes a battery, electronics for controlling the temperature, a heating element (blade), and a cigarette extractor. The heating element heats the tobacco plug in a controlled manner to a maximum temperature of 350 °C. The comparative analytical specifications of the THS2.2 aerosol and 3R4F smoke are reported in part 2 of this series of publications (Schaller et al., 2016-a). The tobacco blend designated 'FR1' was used in the THS2.2 sticks in this study.

2.4. Smoke generation and animal exposure

Aerosol from 3R4F was generated on 30-port rotary smoking machines (Burghart Messtechnik, Wedel, Germany) (15 ports blocked) equipped with a Programmable Dual-port Syringe Pump (PDSP) with an active side stream exhaust (type PMRL-G, SM2000). Aerosol from THS2.2 was generated using 30-port carousel smoking machines (Burghart Messtechnik) equipped with stick holders and a PDSP. Animal exposure is described in detail in Part 4 of this series (Wong et al., 2016). Characterization of test atmospheres showed that target nicotine concentrations were met. Exposure intake was confirmed by quantification of total nicotine metabolites in 24-hour urine (Wong et al., 2016).

2.5. RNA isolation and miRNA profiling

Dissection took place 16 hours after the last exposure. Prior to organ removal, whole-body perfusion with cold saline was performed. The left lung lobe was cryosectioned into 40-μm slices, and the slices were collected alternately for transcriptomics and other analyses (not shown here). Lung samples were lysed in RLT buffer (Qiagen, Hilden, Germany) + β-mercaptoethanol using ceramic beads for homogenization. RNA including miRNA was isolated using the miRNeasy Mini Kit (Qiagen). miRNA was labeled with the FlashTag™ Biotin HSR Labeling Kit (Affymetrix, Santa Clara, CA, USA). miRNA analysis was performed on an Affymetrix GeneChip® miRNA 3.0 Array using 200 ng of RNA as a starting material.

2.6. miRNA data analysis

The raw data were preprocessed through a standard pipeline. Briefly, raw data CEL files were read using the *read.celfiles* function of the oligo packages in the Bioconductor suite of microarray analysis tools available in the R statistical software environment (Carvalho and Irizarry, 2010; Gentleman et al., 2004; R Core Team, 2014). The quality control (QC) was based on the *arrayQualityMetrics* package and examined four distinct metrics: Euclidean distances between arrays in raw and normalized data heat maps, normalized unscaled standard error (NUSE) plots, and intensity distribution box plots (Kauffmann et al., 2009). Arrays that were identified as outliers in at least two of the metrics were discarded, and the QC metrics were recalculated on the remaining arrays until all were accepted. This approach led to seven arrays being discarded in two iterations, so that the number of animal per experimental group decreased from 6 to an average of 5.25 ± 0.79. Normalized probe-level data were obtained by applying robust multiarray normalization and summarized at the probe set level using the median polish method (Irizarry et al., 2003). These miRNA expression data were submitted to ArrayExpress with the accession number E-MTAB-5296.

Only the miRNA probe sets that had significantly higher intensity values than their guanine-cytosine (GC) and sequence length-matched background probes (p-value cut-off = 0.01) were considered to be "present" or "detected," based on the manufacturer's instructions (see the Detection section in the Affymetrix® miRNA QCTool user guide; (Affymetrix, 2011). If a miRNA probe set was detected in more than half of the samples of at least one sample group, it was retained for the downstream analysis; if not, it was discarded together with all of the probe sets measured on the array that belonged to other species than rat. Overall, this preprocessing yielded 321 detected miRNA probe sets in the final expression miRNA matrix. When comparing experimental sample groups (Fig. 1B), the distributions of the numbers of detected miRNAs in individual samples can be used as an indicator of global downregulation. In doing so, we reasonably assume that the downregulation affecting the miRNA probe sets with intensities close to the detection threshold similarly affects all of the detected miRNA probe sets.

The design of our experiment entails 16 pairwise "treatment vs. control" comparisons so as to derive miRNA regulation upon exposure or recovery (e.g. low 3R4F male 90d vs. sham male 90d). For each comparison, a submatrix of the miRNA expression matrix was derived by keeping only the samples belonging to the treatment or control group, as well as the miRNA probe sets that were detected in more than 50% of the samples of at least one of two experimental groups. Linear models for differential expression were applied to the resulting submatrices using the moderated *t*-statistics implemented in the *limma* package (Ritchie et al., 2015). The obtained raw p-values were then adjusted for multiple testing by the Benjamini–Hochberg False Discovery Rate (FDR) method (Benjamini and Hochberg, 1995).

Besides the standard volcano plots (Allison et al., 2006), we used quantile-quantile (Q-Q) plots to represent the global significance of the differential miRNA expression. For each comparison, all of the detected miRNAs were ranked according to decreasing raw p-values. The −log10 values of the corresponding quantiles were plotted on the x-axis, while the y-axis contained the −log10 values of their raw p-values. Deviations of the resulting Q-Q curve above the diagonal line, which represents the random situation, indicate that a global signal was detected in the comparison. To assess the significance of these deviations, we estimated the 95% confidence intervals of each point of the diagonal by calculating the Q-Q curves of 1000 alternative expression matrices obtained by randomly permuting the columns of the original miRNA expression matrix. Merging these 95% confidence intervals yielded the gray surfaces drawn around the diagonal lines on the Q-Q plots. We also added three relevant boundary lines forming a "Z" shape: the lower one delimits the raw p-values smaller than 0.05, the upper one delimits the Bonferroni-corrected p-values smaller than 0.05 (Bonferroni, 1935), and the oblique one joining the other two delimits the Benjamini–Hochberg adjusted p-values (i.e. FDRs) smaller than 0.05 (Benjamini and Hochberg, 1995).

2.7. Quantitative RT-PCR

To confirm the findings from the miRNA experiment, real-time PCR profiling of miRNAs using the miScript PCR System (SYBR®

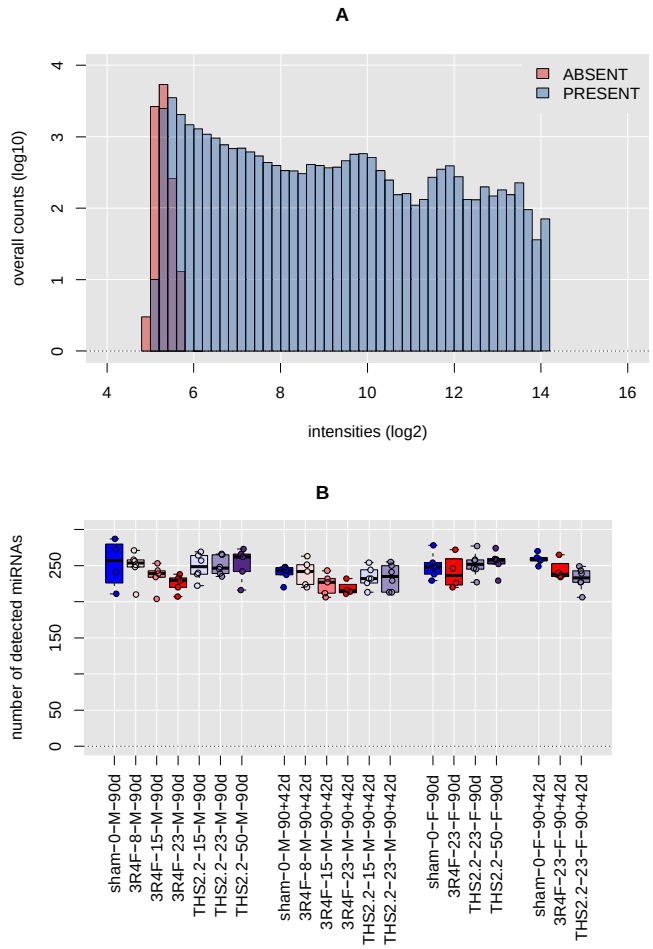

Fig. 1. miRNA detection statistics. A) Histogram displaying the distributions of the miRNA intensities according to their respective detection "present" or "absent" status. The 105 samples and the 321 "present" or "detected" miRNAs were used to generate the figure (see the Materials and Methods section on miRNA data analysis). B) Box plot of the number of "present" miRNAs detected in single samples grouped according to the 20 experimental sample groups included in the design of the study. The box plots follow the standard convention with the bold black horizontal bar representing the distribution median and the surrounding colored rectangle representing its inter-quartile range (i.e. the distance from the first quartile to the third one).

Green-based) was performed. miScript miRNA PCR Arrays are mature miRNA-specific forward primers spotted on a custom 384-well array including controls [SNORD61, SNORD95, positive PCR control (PPC), miRNA reverse transcription control (miRTC)]. The cDNA was prepared by following the manual of the miScript II RT Kit (Qiagen). The qPCR was run in a real-time PCR cycler (Viia7 384-well block). Cq values were then imported into the R environment and processed using the Bioconductor *ReadqPCR* and *NormqPCR* packages (Perkins et al., 2012). δCq values were obtained after subtraction of the mean of the Cq values of two housekeeping genes, SNORD61 and SNORD95. The differential expressions δδCq were calculated using the standard built-in *t*-test function.

Strictly speaking, the selection criterion for the quantitative RT-PCR measurements consisting of a statistically significant difference in expression in at least one of the 16 pairwise comparisons was not met for miR-134 and miR-494. They were nevertheless included in the quantitative RT-PCR measurements because they were very similar to miR-127, miR-379, and miR-541 (see the Results section on genomic clustering of regulated miRNA genes).

2.8. Inference of the changes in the activities of signaling molecules

As described in an accompanying manuscript (Wong et al., 2016), transcriptomic data were generated for the same lung samples as the miRNAs and the corresponding gene differential expression values were calculated using the same statistical models as for the miRNAs. A concise summary of the results obtained for the biological processes relevant for miR-146a/b and miR-182 is provided in Supplementary Fig. 1 in order to further support the conclusions based on these miRNAs. In the present study we used the systems biology approach called Network Perturbation Amplitude (NPA) and more specifically its *Strength* algorithm to infer the changes in the activities of several signaling molecules relevant to this context (Martin et al., 2012). This approach is based on backward causal reasoning, which consists of calculating the changes in the activity of upstream signaling molecules based on the differential expression of the downstream transcripts they causally regulate. For a given protein, the list of its causally regulated transcripts was extracted from Selventa Knowledgebase, which is a comprehensive repository of signed causal relationships between biological entities derived from peer-reviewed scientific literature as well as public and proprietary databases (Catlett et al., 2013). For the sake of clarity, we replaced the abstract openBEL syntax with the corresponding protein names and merged the entities related to the same protein, such as abundances and transcriptional activities. Given the set of signed relationships with downstream transcripts, the changes in the activity of a specific protein inferred by the NPA approach can be quantitatively contrasted across multiple pairwise comparisons, very much like transcript or miRNA differential expression. The obtained NPA values are also accompanied by two statistics that allow quantification of their uncertainty regarding biological variability and their specificity with respect to the choice of the downstream transcripts (Martin et al., 2012).

3. Results

3.1. miRNA detection statistics in lung tissue of rats exposed to CC smoke or THS2.2 aerosol

We first examined the miRNA detection statistics on the Affymetrix GeneChip miRNA-3.0 Microarray. Fig. 1A shows the overall distribution of the single miRNA intensities grouped according to their corresponding "present" or "absent" detection values. This figure confirms that the detection statistics correctly separated the low-intensity values, which cannot be distinguished from the background noise and are not informative, from the higher-intensity signals, for use in drawing conclusions in our study.

Fig. 1B displays the numbers of detected miRNAs across the experimental sample groups. First, CC smoke exposure induced a significant dose-dependent decrease in the number of miRNAs detected in lung tissue, as seen by the median values of 260, 255, 240, and 230 for the male rats exposed to *sham*, *low*, *medium*, and *high* doses of CC smoke, respectively. Second, these differences were still observed 42 days after the cessation of CC smoke exposure with approximately the same magnitude. Third, THS2.2 exposure did not lead to a decrease in the number of detected miRNAs. The distributions found for the lung tissue of the female rats displayed a tendency similar to that found in the male rats, although the fact that not all doses were available made it more difficult to draw firm conclusions (see the Materials and Methods section on experimental design).

3.2. miRNome-wide response in lung tissue of rats exposed to CC smoke or THS2.2 aerosol

We display the miRNome-wide response of the exposed lung tissues using volcano and Q-Q plots (see Fig. 2 for males and Supplementary Fig. 2 for females). They provide a useful overview of the magnitude and statistical significance of the responses that occurred in lung tissue. Volcano plots are standard representations of differential gene expression, while Q-Q plots are normally used in statistical genetics and essentially reveal how different the obtained results are from an undetectable signal. More details about the Q-Q plots are given in the Materials and Methods section on miRNA data analysis.

For the rats exposed to three doses of 3R4F, the volcano plots show that the magnitude of the effect (x-axis) increased with concentration together with the associated statistical significance (first row of the figure, left-hand side). We also observed that only a limited number of miRNAs reached the 0.05 false discovery rate (FDR) threshold for statistically significant regulation (miR-150, miR-146b, miR-182, miR-652). This rather weak signal was also visible in the Q-Q plots with the corresponding points situated above the Benjamini–Hochberg line (second row, left-hand side). However, the clear deviation of the curve of raw p-values from the diagonal toward the upper confidence interval boundary indicates that the measured responses were not random. The Q-Q plots of the comparisons of the 3R4F recovery samples presented similar results for the medium and high 3R4F concentrations, exemplified by a few miRNAs situated immediately below the FDR threshold (fourth row, left-hand side). On the other side, the effects on rats exposed to low 3R4F concentration had disappeared after 42 days of postexposure recovery, as indicated by the raw p-value curve closely following the diagonal, as well as a flat volcano plot. Regarding the global effects of the THS2.2 aerosol after 90 days of exposure, we found no statistically significant differences in miRNA

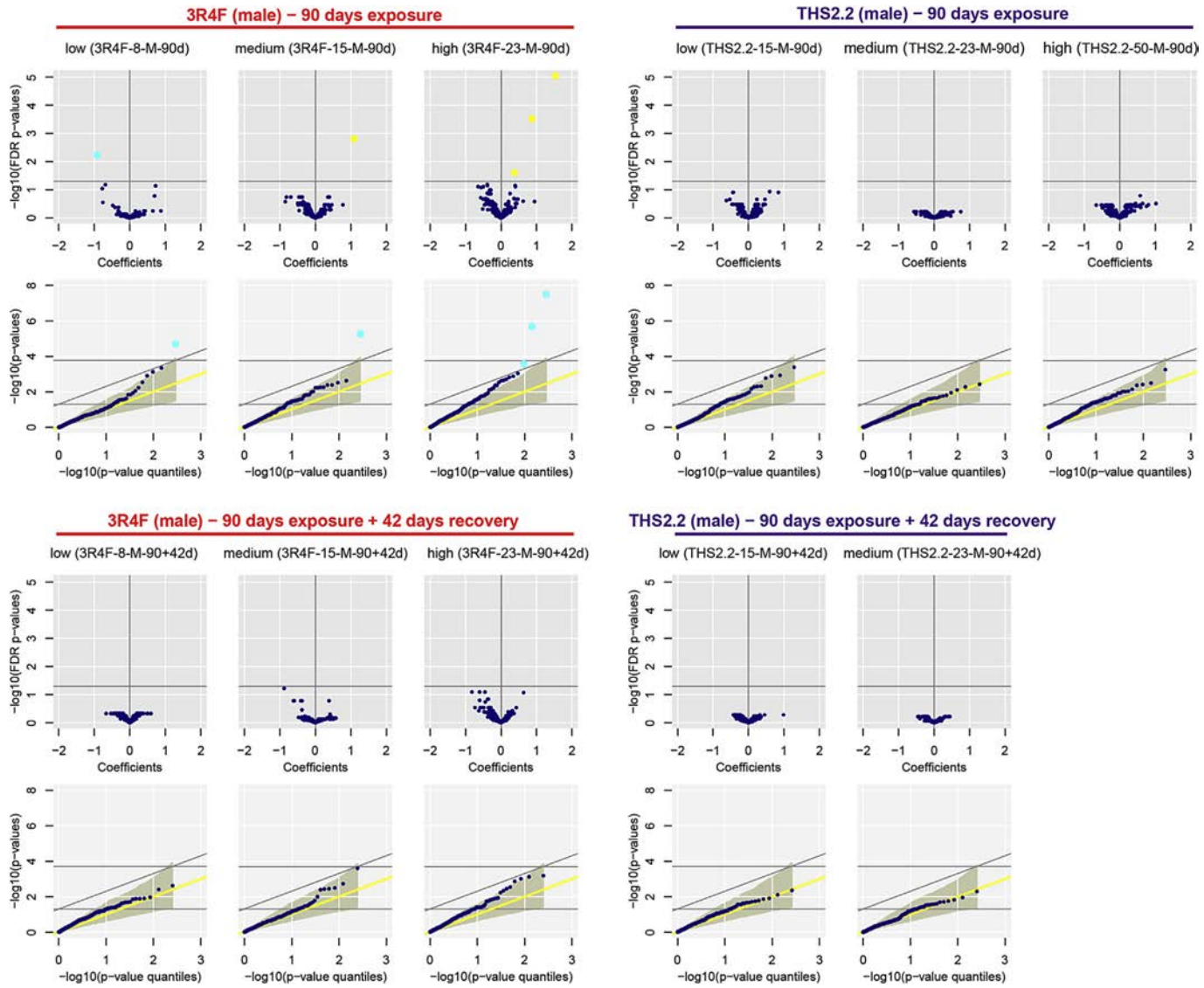

Fig. 2. Global miRNA regulation in male rats. Volcano and Q-Q plots are shown for the 11 pairwise comparisons between CS or THS2.2-exposed male rats and sham-exposed male rats. Volcano plots display the global relationships between the treatment-induced effects (differential miRNA expression, horizontal x-axis) and their statistical significance (log10 FDR, y-axis). Blue (yellow) dots indicate statistically significant negative (positive) regulation (FDR < 0.05). Q-Q plots indicate how distant the global statistical significance of differential miRNA expression (all of the bold-faced points) is from the random case containing no signal (diagonal line). The construction of a Q-Q plot is described in the Materials and Methods section on miRNA data analysis. Blue dots indicate statistically significant regulation of either sign (FDR < 0.05).

expression (first and second rows, right-hand side). Although the corresponding raw p-value curves did not strictly follow the diagonals of the Q-Q plots, the amplitudes of their deviations did not display monotonic dose dependence, which suggests that these effects were too noisy to be correctly interpreted. Finally, very similarly to the results seen after exposure to a low concentration of 3R4F, no effects of THS2.2 aerosol exposure were detected in the recovery group (90 + 42d) (third and fourth rows, right-hand side).

3.3. miRNAs with a statistically significant difference in expression in lung tissue of rats exposed to CC smoke or THS2.2 aerosol

All miRNAs that showed a statistically significant (i.e., FDR <0.05) difference in abundance in at least one exposure group compared with the sham group are shown in Fig. 3A (miR−150, miR−146a/b, miR−182, miR−652, miR−224, miR−181c, miR−127, miR−379, miR−541, miR−30b, miR−125a, miR−139). These data are from microarrays in an exploratory phase, which allowed identification of the key responders to the exposures. For confirmation, the levels of a subset of them were reexamined using quantitative RT-PCR (Pritchard et al., 2012). We selected 10 key miRNAs, the responses of which displayed appropriate dose dependences that were similar in male and female rats. We focused on miR-146a/b, miR-182, miR-127, miR-134, miR-379, miR-494, and miR-541 because they showed, to a certain degree, concentration-dependent regulation that was independent of sex. miR-139 was included as a potential recovery marker, while miR-150 seemed to capture low-dose effects. Supplementary Fig. 4 (intensity distributions) and 3B (differential expression) show the results of confirmatory phase by quantitative RT-PCR.

Quantitative RT-PCR results confirmed that the two paralogous miR-146a/b were upregulated both in response to 3R4F smoke exposure and after the recovery period, albeit at a lower intensity (Fig. 3B). In the lungs of female rats, miR-146b displayed a stronger response, which was also manifested by weak but statistically significant upregulation in female rat lungs upon THS2.2 exposure. miR-182 was upregulated in the lungs of both male and female rats exposed to 3R4F smoke, but not in the recovery groups. miR-127, miR-134, miR-379, miR-494, and miR-541 collectively displayed clear downregulation in both the 3R4F smoke exposure and recovery groups, as well as upregulation in the THS2.2 aerosol exposure groups. This upregulation was not observed in the recovery group of THS2.2-exposed rats. miR-139 and miR-150 displayed almost no signal in the quantitative RT-PCR results, so we considered them to be false positives in the microarray analysis. Except for these two miRNAs, the quantitative RT-PCR results accurately confirmed the microarray observations (Supplementary Fig. 5).

3.4. Mechanistic insight into miRNA regulation using transcriptomic data

We next aimed to obtain further insight into the mechanisms leading to regulation of the miRNAs in the exposed rat lung tissue. In the literature, it is indicated that miR-146a/b function as negative regulators involved in downregulation of Interleukin 1 (IL-1) receptor-associated kinase 1 (IRAK1) and tumor necrosis factor (TNF) receptor-associated factor 6 protein levels (TRAF6) and that miR-146a/b induction is NFkB-dependent (Taganov et al., 2006). As an alternative pathway, miRNA-146a was described to be induced by IL-1β in alveolar epithelial cells, where the upregulation of miR-146a/b resulted in the suppression of RANTES and IL-8 (Perry et al., 2008). It was further shown that miR-146a and miR-146b were regulated via divergent intracellular pathways. Upon stimulation with IL-1β, miR-146a induction was regulated via an NFkB- and JNK-1/2-dependent mechanism, and miR-146b was regulated via a JNK-1/2- and MEK-1/2-dependent mechanism (Perry et al., 2009).

In the absence of protein activity data, we used a previously reported approach to infer the activities of these signaling molecules based on the transcriptomic data (Fig. 4A and the section

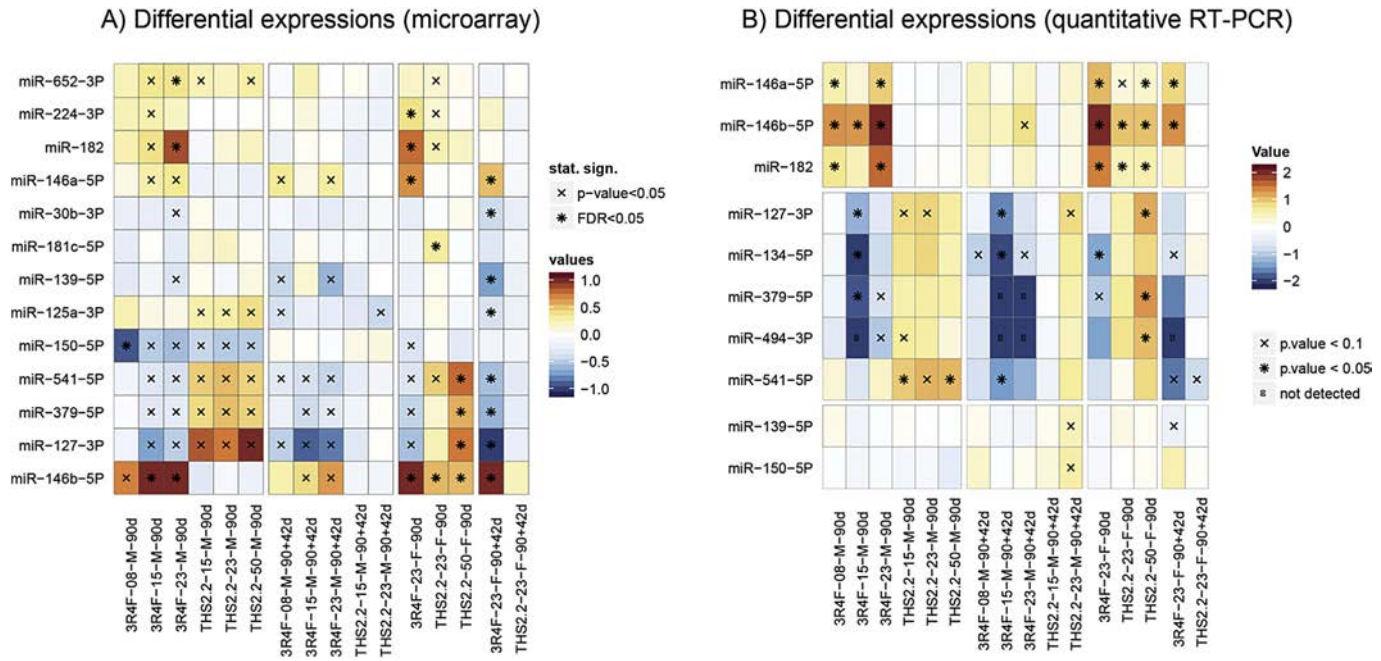

Fig. 3. Regulation of individual miRNAs (all pairwise comparisons). Heat maps display the regulation and the associated statistical significance for the relevant miRNAs. A) Results from the microarray exploratory measurements; only the miRNAs that have an FDR value below 0.05 in at least one of the 16 pairwise comparisons are shown. The miRNAs were ordered by standard clustering. B) Results from the confirmatory quantitative RT-PCR measurements for 10 selected miRNAs. The miRNAs have been grouped according to the considerations explained in the text.

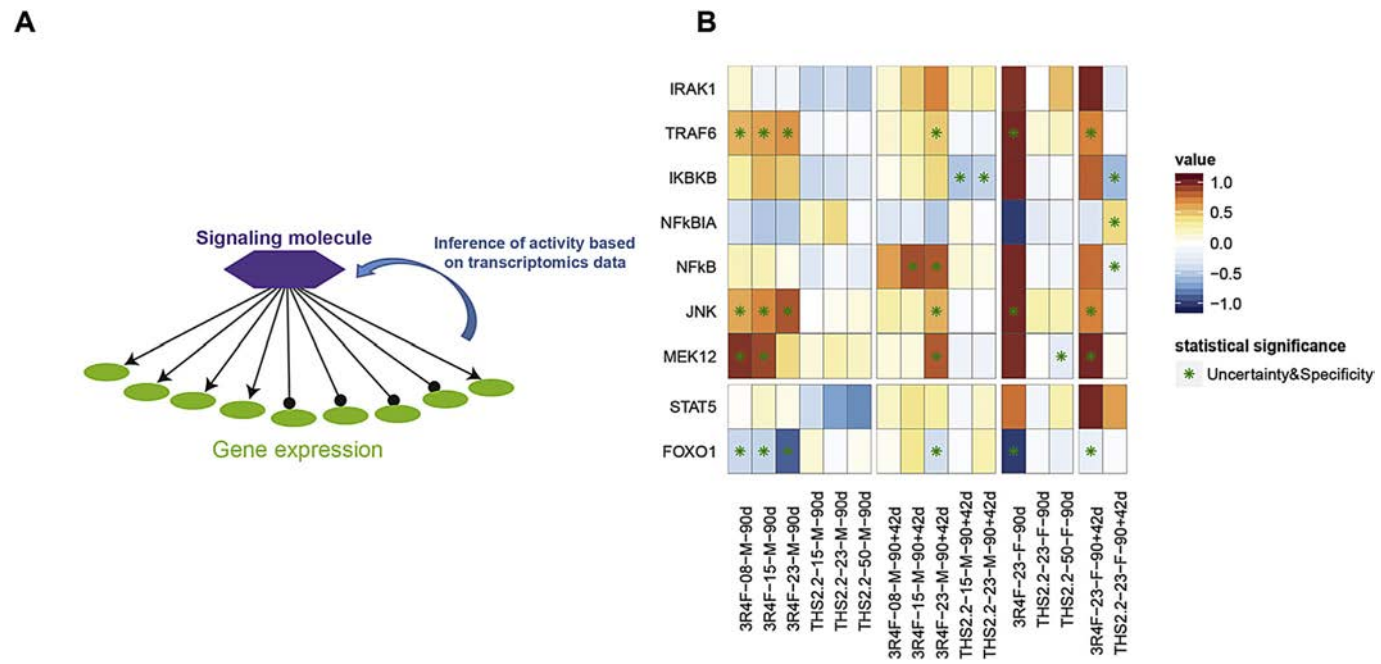

Fig. 4. Mechanistic insight into miRNA regulation using transcriptomic data. A) The principle of inference of the regulation of different signaling components based on transcriptomic data. The differential gene expression in the dataset was used for backward reasoning to infer the regulation of signaling molecules (purple polygon) known to regulate gene expression (green balls). The inference algorithm provides two statistics. Uncertainty measures the experimental variability and specificity requires that the correct genes are regulated in the dataset and that the downstream genes cannot be replaced with a random set of regulated genes. The method inferring the displayed values is described in Materials and Methods. B) The heat map shows the inferred regulation of signaling components known to be causally upstream or downstream of miR-146a/b and miR-182. The transcriptomic data from rat lung were used to infer the activity of the chosen molecules. The information on the gene regulation downstream of these signaling molecules is derived from experimental evidence stored in the Selventa knowledgebase.

about the inference of changes in the activities of signaling molecules in Materials and Methods). Fig. 4B shows the inferred activation or inhibition of the components involved in miR-146a/b signaling based on transcriptomic data. NFkB was inferred to be significantly upregulated only in the male recovery group, but the strong inferred upregulation of NFkB, observed in both exposure and recovery groups in females, did not reach statistical significance. By contrast, NFkB was significantly downregulated in the recovery group of females exposed to THS2.2. The kinase (IKBKB) that targets the inhibitor of NFkB (NFkBIA) to be degraded was predicted to be downregulated in the recovery groups of both sexes after exposure to THS2.2. Accordingly, NFkBIA was inferred to be upregulated in the recovery group of female rats exposed to THS2.2, consistent with the observation that the activity of NFkB was inferred to be downregulated in this group. The miR-146 target TRAF6 was inferred to be strongly upregulated and IRAK1 was only impacted in females with even stronger upregulation in the recovery groups for both sexes. The impact of THS2.2 exposure was significantly reduced compared with that of 3R4F exposure.

The inferred activation of JNK-1/2 was concentration-dependent, present in both sexes, and displayed a statistically significant effect at 90 days, with a smaller impact on the lungs of rats in the recovery group. The impact of THS2.2 exposure was significantly reduced compared with that of 3R4F exposure. MEK-1/2 was inferred to be less activated when the CC smoke concentration increased in the male rat lungs in response to 3R4F exposure at 90 days and in the recovery group exposed to the highest dose of 3R4F. In female rat lungs, it was inferred to be downregulated in the THS2.2-exposed group at 90 days and upregulated in the recovery group after 3R4F exposure (Fig. 4B).

miRNA-182 has been shown to be induced by STAT5, which is activated via the IL-2 pathway, in the context of the transition of naïve helper T cells to clonal expansion (O'Neill, 2010). To determine whether this could also be true in lung tissue, we inferred the activities of STAT5 and FOXO1 based on transcriptomic data. STAT5 was not inferred to be activated in CC smoke-exposed rat lungs, or even in the recovery groups. However, FOXO1 was predicted to be significantly downregulated in response to 3R4F exposure in both male and female rat lungs compared with that in the sham rats. This downregulation was also present, albeit at a lower level, in the recovery groups (Fig. 4B). In the lungs of rats exposed to THS2.2 aerosol, no consistent trends were observed for the inferred regulation of the signaling components.

3.5. Genomic clustering of regulated miRNA genes

When selecting miR-127, miR-134, miR-379, miR-494, and miR-541 for quantitative RT-PCR confirmation (Fig. 3B), we noticed that they are all located within 200 kilobases of each other on chromosome 6, in a region known as the DLK1-DIO3 imprinted domain situated in band 6q32 (da Rocha et al., 2008). Only the maternal copy of chromosome 6 expresses the miRNAs, which are organized into two large clusters regulated by an intergenic differentially methylated region located between Dlk1 and RGD1566401 (or MEG3/GTL2) (Fig. 5A). Since these features are also present in mouse and human on chromosomes 12 and 14, respectively, we decided to investigate in more detail the responses of the detected miRNAs located in this region as captured by the microarray. Fig. 5B shows that, besides the five above-mentioned ones, 19 other mature miRNAs were detected in at least one of the 16 pairwise comparisons in the study. Given that the total number of precursor miRNAs provided by RefSeq for this region is greater than 50 (Pruitt et al., 2014), our results indicate that the transcription of genomically clustered miRNAs was not necessarily as uniform as one might have expected (Baskerville and Bartel, 2005). More specifically, only a fraction of the detected miRNAs displayed a signal that was strong

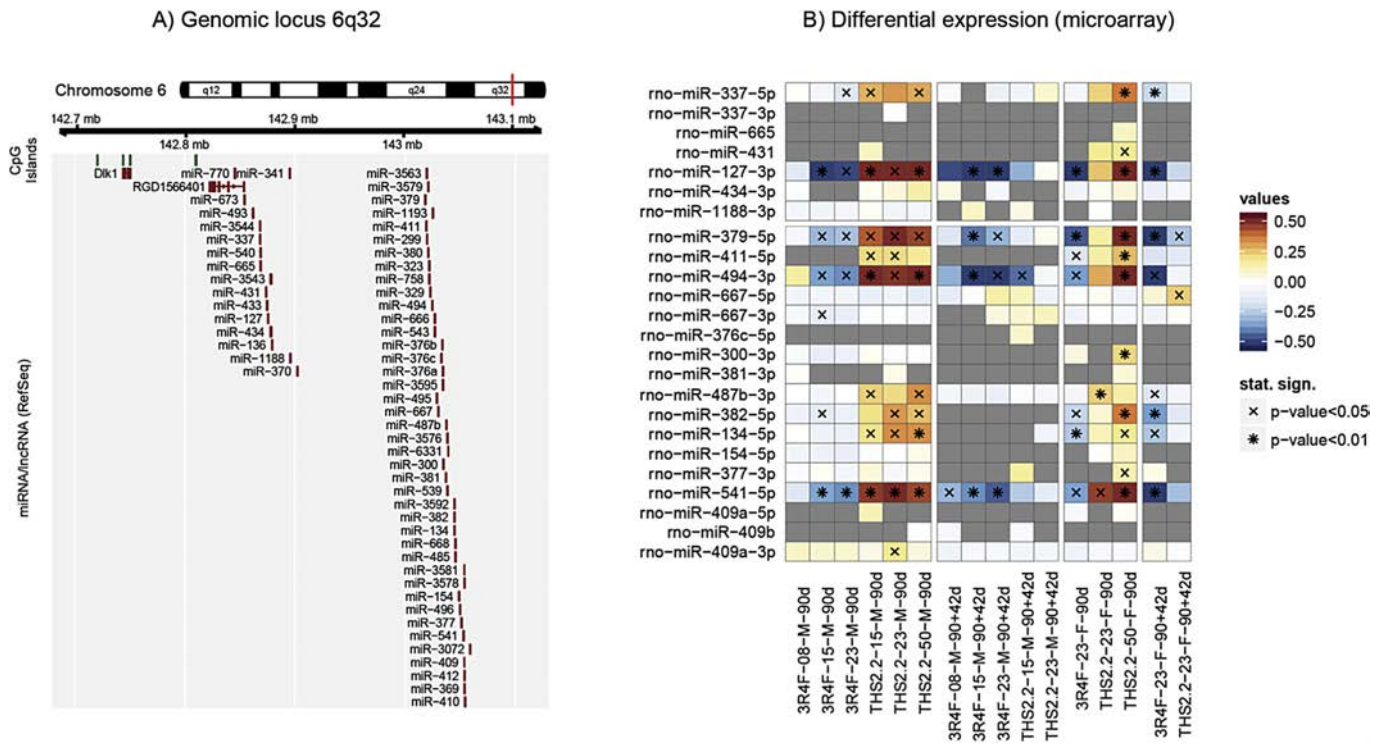

Fig. 5. miRNAs in the DLK1-DIO3 cluster. A) Genomic map of the imprinted DLK1-DIO3 cluster located on rat chromosome 6. CpG islands have been included beside the miRNAs and the long noncoding RNA genes (lncRNAs), as they play an important role in the imprinting mechanism. B) Regulation of all of the detected miRNAs in the DLK1-DIO3 cluster. Note that the criteria for indicating the "statistical significance" on the heat map are different from the ones used on Fig. 3A.

enough to deduce a response profile that could be compared with those of the five already-selected ones. miR-337 and miR-382 approximately displayed both the CC smoke-induced downregulation and the THS2.2-induced upregulation observed in Fig. 3, while miR-411 and miR-487b displayed only the THS2.2-induced upregulation. All of the others displayed a signal that was too weak to draw any definitive conclusions.

4. Discussion

4.1. miRNA detection: global downregulation upon CC smoke exposure

Our observation of a decreased number of detected miRNAs upon CC smoke exposure (Fig. 1B) can be viewed as an indicator of the global downregulation of miRNAs (see the Materials and Methods section on miRNA data analysis). The use of detection statistics has the advantage of being independent of the microarray raw data normalization method, which might reduce such global downregulation effects (Sewer et al., 2014). We also concede that our approach based on detection calls is useful only as long as the global effects between experimental sample groups are larger than the corresponding within-group variabilities. Fortunately, this is predominantly the case in the present study, as can be seen by comparing the within-group interquartile ranges and the between-group median differences in the boxplots of Fig. 1B.

The phenomenon of the global downregulation of miRNAs has already been reported in the literature, initially in disease (mostly cancer) contexts (Izzotti and Pulliero, 2014; Wu et al., 2013), but more recently also in the toxicological context of healthy organisms or systems, particularly after exposure to CC smoke (Graff et al., 2012; Izzotti et al., 2009b; Mathis et al., 2013; Schembri et al., 2009; Sewer et al., 2014). Several mechanisms have been proposed to explain this. Suzuki et al. showed that some toxicants can cause DNA damage and the activation of P53, which interacts with the DROSHA/DGCR8 processing complex and thus modulates the processing of pri-miRNAs to pre-miRNAs (Suzuki and Miyazono, 2010; Suzuki et al., 2009). Another possibility is that several toxicants can form miRNA adducts, which modify the structure of the miRNAs and prevent their access to the catalytic pockets of Dicer, thus arresting their maturation process (Izzotti and Pulliero, 2014). Alternatively, some toxicants can bind to Dicer in the proximity of miRNA catalytic sites and block the maturation of miRNA precursors (Ligorio et al., 2011). This scenario was investigated in detail in the case of alveolar macrophages obtained from healthy smokers and revealed the specific mechanism of Dicer SUMOylation (Gross et al., 2014).

Our observations of a dose-dependent decrease in the number of detected miRNAs upon CC smoke exposure are evidently compatible with all of these explanations. However, more interesting is the fact that (almost) no changes were detected in the recovery groups, which indicates that P53 and/or some CC smoke toxicants were persistently interfering with the miRNA processing machinery. On the other hand, regarding evaluation of the impact of the THS2.2 heat-not-burn product, the absence of any signs of global downregulation of miRNAs constitutes initial evidence of a lower impact of its aerosol in the lung and that the miRNA processing machinery was not affected by the various mechanisms that we described in the case of CC smoke exposure.

4.2. Overall miRNA regulation in response to CC smoke exposure

The global miRNA regulation results revealed several fundamental features of the miRNA response, such as the approximately monotonic dose dependence, the sustained 3R4F effects after exposure cessation, and no (males) or low (females) impact of

THS2.2 (Fig. 2). However, the number of miRNAs that showed a statistically significant difference in their expression level was rather low, even in response to 3R4F exposure. The first reason for this is our choice of separate comparisons for male and female rats. To verify the sensitivity of the study, we tested an alternative statistical model merging both sexes and encoding the animal sex into a discrete covariate. On average, the results contained three to four times more miRNAs that showed a statistically significant difference in their expression levels and confirmed the features enumerated above (Supplementary Fig. 3). In our data processing pipeline described in the Materials and Methods section on miRNA data analysis, we also minimized the effects of multiple testing corrections by restricting the statistical analysis of each comparison to the miRNAs that were detected in the majority of samples in at least one sample group.

To obtain a better understanding of the global miRNA regulation in response to CC smoke or THS2.2 aerosol exposure, we complemented the standard volcano plot of each pairwise comparison with the corresponding Q-Q plot. This has several advantages, the most important of which is the ability of this latter plot to explicitly display the case of a random dataset, which cannot be achieved with a volcano plot. Note that the diagonal corresponds to the random case under the assumption that all miRNAs are independent (uncorrelated), which might be invalid in the case of coexpressed miRNAs (clustered and/or polycistronic). Another advantage is the fact that a Q-Q plot focuses on the raw p-values rather than the FDRs. Raw p-values better reflect the key factors to reach statistical significance: the measured effect size and its variability, as well as the experimental sensitivity resulting from its design (number of replicates).

Regarding the assessment of THS2.2, a better understanding of its reduced impact in lung tissue compared with CC smoke can be obtained by examining the individual miRNAs below.

4.3. Mechanistic insights into miRNA regulation in exposed rat lung

Previous observations showed a relatively poor correlation of miRNA regulation between different studies (Vrijens et al., 2015). Pertinent to our study, miR-146a/b was previously reported to be downregulated in mouse lungs in response to short-term CC smoke exposure (Izzotti et al., 2010; Izzotti and Pulliero, 2014). However, other studies showed the upregulation of miRNA in inflammatory conditions, such as IL-1β-induced alveolar cells (Perry et al., 2008), in a mouse model of ventilator-induced lung injury (Vaporidi et al., 2012) and by proinflammatory cytokines in human airway smooth muscle (Comer et al., 2014). This suggests that, while toxicant exposure is generally thought to induce downregulation of miR-146a/b, the situation may change when tissue homeostasis is compromised. Based on the targets identified for miR-146a/b, they are thought to function as negative regulators of inflammatory responses (Saba et al., 2014). Since we could not infer downregulation of the miR-146a/b targets IRAK1 and TRAF6, one could hypothesize that the inflammatory status of the rat lung had already reached a high level that could not be inhibited by the negative regulation by miR-146a/b, even though it was induced in the lung tissue. The hypothesis on the involvement of the NFkB pathway in miR-146a/b regulation in CC smoke-exposed rat lungs could also not be confirmed. However, the strong inferred upregulation of NFkB in the male recovery group might indicate its involvement in the tissue healing process, independent of the miR-146 pathway. On the other hand, JNK-1/2 and MEK-1/2 upstream of miR-146a/b were inferred to be activated, based on transcriptomic data.

It has been reported that STAT5 is a direct activator of miR-182, which is in turn a robust inhibitor of FOXO1 (O'Neill, 2010), and that oxidative stress may inactivate STAT5 in a JAK2-independent manner (Saba et al., 2014). In CC smoke-exposed rat lungs, we observed that the upregulation of miR-182 was accompanied by strong downregulation of FOXO1. However, STAT5, which has been suggested to be involved upstream of the miR-182 FOXO1 pathway, was not impacted in response to CC smoke exposure in rat lung. This indicates that miR-182 could be regulated via other signaling pathways in the inflamed lung. A potential upstream candidate is STAT3 as a chromatine immunoprecipitation (ChIP) assay revealed that, upon autocrine HGH stimulation, STAT3 and STAT5 directly bind to the promoter region of the miR-96-182-183 cluster (Zhang et al., 2015), and indeed our data suggested that STAT3 was upregulated (data not shown). However, experimental results are needed to confirm this.

After 90 days of THS2.2 exposure, neither miR-146 nor miR-182 was impacted. In line with this, the gene expression-based inference did not predict any significant activations or inhibitions.

Regarding all of the negative findings concerning the hypotheses based on the literature about miR-146 and miR-182 regulatory pathways, it is also possible that, at present, we cannot capture the activation of all components in the signaling pathways. Thus, more controlled experiments are deemed necessary to fully elucidate the function of these miRNA species in the context of pulmonary inflammation.

4.4. miRNAs from the DLK1-DIO3 miRNA cluster

miRNA genes are often clustered in the genome and show similar spatiotemporal regulation, which results from coregulation and even cotranscription (Baskerville and Bartel, 2005). In this study, we saw that several miRNAs from the large DLK1-DIO3 miRNA cluster shared a noteworthy response pattern: they were downregulated upon CC smoke exposure and upregulated upon THS2.2 exposure. The fact that downregulation often corresponded to the absence of detection in both exploratory microarray and confirmatory quantitative RT-PCR measurements indicated that this signal was very weak and unlikely to be present in all of the cellular types constituting the “whole lung” samples. The cells that drive the observed signal might be macrophages. Indeed, it has been shown that CC smoke exposure induces inverse M1 and/or M2 polarization states (Shaykhiev et al., 2009; Titz et al., 2015), and that M2-polarized macrophages exhibit lower levels of miR-127 (Zhang et al., 2013). These two observations agree with the CC smoke part of our findings. Mechanistically, even a role for miR-127 in the context of macrophage polarization was identified (Ying et al., 2015). This suggests that lower miR-127 levels induce an M2-biased response, which fits well with our findings. We observed the clear upregulation of numerous miRNAs belonging to the DLK1-DIO3 miRNA cluster upon THS2.2 exposure. Such a collective effect has already been observed for the human homologous miRNAs and explained in that context by the hypomethylation of upstream CpG islands, which might match the ones shown in Fig. 5A (Aavik et al., 2015).

5. Conclusion

Investigations on the miRNA response to CC smoke exposure have drawn significant interest in recent years, so we wanted to cast our comparative THS2.2 assessment into this context. Systems toxicology tools offered the possibility of inferring upstream and downstream protein activities using our transcriptomic data obtained from the same samples, which provided an additional layer of understanding of the effects of CC smoke and THS2.2. In conclusion, the current study showed that subchronic CC smoke exposure induces global miRNA downregulation in rat lung, which

is probably linked to reactive CC smoke constituents interfering with the miRNA processing machinery. The upregulation of specific miRNA species, such as miR-146a/b and miR-182, indicates that they are causal elements in the inflammatory response in CS-exposed lung. This study also shows that exposure to THS2.2 did not result in effects similar to those observed upon exposure to the reference cigarette.

Conflict of interest statement

The work reported in this publication involved a candidate Modified-Risk Tobacco Product developed by Philip Morris International (PMI) and was solely funded by PMI. All authors are (or were) employees of PMI R&D or worked for PMI R&D under contractual agreements.

Acknowledgements

The authors would like to thank the study team, especially acknowledging the technical assistance and support of the bioresearch and aerosol team at PMI Research Laboratories Singapore particularly Wong Sin Kei, Nigel Tan, Aaron Ong, Woon Ching Qing, Clement Foong, Jenny Ho, Eleena Seow, Subash Krishnan and Shen Yi. We acknowledge the technical assistance for lung slicing, RNA isolation and gene chip preparation provided by Abdelkader Benyagoub, Karine Baumer, Dariusz Peric and Remi Dulize, respectively. We thank Dr. Walter Schlage for his scientific input and critical review of the manuscript.

Transparency document

Transparency document related to this article can be found online at http://dx.doi.org/10.1016/j.yrtph.2016.11.018.

Appendix A. Supplementary data

Supplementary data related to this article can be found at http://dx.doi.org/10.1016/j.yrtph.2016.11.018.

References

Aavik, E., et al., 21 April 2015. Global DNA methylation analysis of human atherosclerotic plaques reveals extensive genomic hypomethylation and reactivation at imprinted locus 14q32 involving induction of a miRNA cluster. Eur. heart J. 36 (16) ehu437.
Affymetrix, 2011. Affymetrix miRNA QCTool User's Guide.
Allison, D.B., et al., 2006. Microarray data analysis: from disarray to consolidation and consensus. Nat. Rev. Genet. 7, 55–65.
Baskerville, S., Bartel, D.P., 2005. Microarray profiling of microRNAs reveals frequent coexpression with neighboring miRNAs and host genes. Rna 11, 241–247.
Benjamini, Y., Hochberg, Y., 1995. Controlling the false discovery rate: a practical and powerful approach to multiple testing. J. R. Stat. Soc. Ser. B Methodol. 289–300.
Bonferroni, C.E., 1935. Il calcolo delle assicurazioni su gruppi di teste. Tipografia del Senato.
Carvalho, B.S., Irizarry, R.A., 2010. A framework for oligonucleotide microarray preprocessing. Bioinformatics 26, 2363–2367.
Catlett, N.L., et al., 2013. Reverse causal reasoning: applying qualitative causal knowledge to the interpretation of high-throughput data. BMC Bioinforma. 14, 1.
Comer, B.S., et al., 2014. MicroRNA-146a and microRNA-146b expression and anti-inflammatory function in human airway smooth muscle. Am. J. Physiol. Lung Cell. Mol. Physiol. 307, L727–L734.
da Rocha, S.T., et al., 2008. Genomic imprinting at the mammalian Dlk1-Dio3 domain. Trends Genet. 24, 306–316.
De Smet, E.G., et al., 2015. Non-coding RNAs in the pathogenesis of COPD. Thorax. thoraxjnl 70 (8), 782–791, 2014–206560.
Family Smoking Prevention and Tobacco Control Act. Public Law No. 111–131 (June 22, 2009).
Gentleman, R.C., et al., 2004. Bioconductor: open software development for computational biology and bioinformatics. Genome Biol. 5, R80.
Graff, J.W., et al., 2012. Cigarette Smoking Decreases Global MicroRNA Expression in Human Alveolar Macrophages.
Gross, T.J., et al., 2014. A microRNA processing defect in smokers' macrophages is linked to SUMOylation of the endonuclease DICER. J. Biol. Chem. 289, 12823–12834.
Haziza, C., 2016. Evaluation of the Tobacco Heating System 2.2. Part 8: 5–Day Randomized Reduced Exposure Clinical Trial in Poland. Regul. Toxicol. Pharmacol. 81 (S2), S139–S150.
Hong, W.Y., Cho, W.C., 2015. The role of microRNAs in toxicology. Arch. Toxicol. 89, 319–325.
Irizarry, R.A., et al., 2003. Summaries of Affymetrix GeneChip probe level data. Nucleic acids Res. 31 e15–e15.
Izzotti, A., et al., 2009a. Downregulation of microRNA expression in the lungs of rats exposed to cigarette smoke. FASEB J. 23 (3), 806–812.
Izzotti, A., et al., 2009b. Relationships of microRNA expression in mouse lung with age and exposure to cigarette smoke and light. FASEB J. 23, 3243–3250.
Izzotti, A., et al., 2010. Modulation of microRNA expression by budesonide, phenethyl isothiocyanate and cigarette smoke in mouse liver and lung. Carcinogenesis 31, 894–901.
Izzotti, A., Pulliero, A., 2014. The effects of environmental chemical carcinogens on the microRNA machinery. Int. J. Hyg. Environ. health 217, 601–627.
Kauffmann, A., et al., 2009. arrayQualityMetrics—a bioconductor package for quality assessment of microarray data. Bioinformatics 25, 415–416.
Kogel, U., et al., 2016. Evaluation of the Tobacco Heating System 2.2. Part 7: Systems Toxicological Assessment of a Mentholated Version Revealed Reduced Cellular and Molecular Exposure Effects Compared with Mentholated and Non-mentholated Cigarette Smoke. Regul. Toxicol. Pharmacol. 81 (S2), S123–S138.
Krol, J., et al., 2010. The widespread regulation of microRNA biogenesis, function and decay. Nat. Rev. Genet. 11, 597.
Lema, C., Cunningham, M.J., 2010. MicroRNAs and their implications in toxicological research. Toxicol. Lett. 198, 100–105.
Ligorio, M., et al., 2011. Mutagens interfere with microRNA maturation by inhibiting DICER. An in silico biology analysis. Mutat. Res. Fundam. Mol. Mech. Mutagen. 717, 116–128.
Liu, X., et al., 2009. Uncovering growth-suppressive MicroRNAs in lung cancer. Clin. Cancer Res. 15, 1177–1183.
Luettich, K., et al., 2014. Systems toxicology approaches enable mechanistic comparison of spontaneous and cigarette smoke-related lung tumor development in the A/J mouse model. Interdiscip. Toxicol. 7, 73–84.
Martin, F., et al., 2014. Quantification of biological network perturbations for mechanistic insight and diagnostics using two-layer causal models. BMC Bioinforma. 15, 1.
Martin, F., et al., 2016. Evaluation of the Tobacco Heating System 2.2. Part 9: Application of Systems Pharmacology to Identify Exposure Response Markers in Periferal Blood of Smokers Switching to THS2.2. Regul. Toxicol. Pharmacol. 81 (S2), S151–S157.
Martin, F., et al., 2012. Assessment of network perturbation amplitudes by applying high-throughput data to causal biological networks. BMC Syst. Biol. 6, 54.
Mathis, C., et al., 2013. Human bronchial epithelial cells exposed in vitro to cigarette smoke at the air-liquid interface resemble bronchial epithelium from human smokers. Am. J. Physiol. Lung Cell. Mol. Physiol. 304, L489–L503.
NACLAR, 2004. (National Advisory Committee for Laboratory Animal Research): guidelines on the Care and Use of Animals for Scientific Purposes.
O'Neill, L.A., 2010. Outfoxing Foxo1 with miR-182. Nat. Immunol. 11, 983–984.
Oviedo, A., et al., 2016. Evaluation of the Tobacco Heating System 2.2. Part 6: 90-day OECD 413 Rat Inhalation Study with Systems Toxicology Endpoints Demonstrates Reduced Exposure Effects of a Mentholated Version Compared with Mentholated and Non-mentholated Cigarette Smoke. Regul. Toxicol. Pharmacol. 81 (S2), S93–S122.
Perkins, J.R., et al., 2012. ReadqPCR and NormqPCR: R packages for the reading, quality checking and normalisation of RT-qPCR quantification cycle (Cq) data. BMC genomics 13, 296.
Perry, M.M., et al., 2008. Rapid changes in microRNA-146a expression negatively regulate the IL-1β-induced inflammatory response in human lung alveolar epithelial cells. J. Immunol. 180, 5689–5698.
Perry, M.M., et al., 2009. Divergent intracellular pathways regulate interleukin-1β-induced miR-146a and miR-146b expression and chemokine release in human alveolar epithelial cells. FEBS Lett. 583, 3349–3355.
Pritchard, C.C., et al., 2012. MicroRNA profiling: approaches and considerations. Nat. Rev. Genet. 13, 358–369.
Pruitt, K.D., et al., 2014. RefSeq: an update on mammalian reference sequences. Nucleic acids Res. 42, D756–D763.
R Core Team, 2012. R: a Language and Environment for Statistical Computing. R Foundation for Statistical Computing, Vienna, Austria. ISBN 3-900051-07-0, 2014.
Ritchie, M.E., et al., 20 April 2015. Limma powers differential expression analyses for RNA-sequencing and microarray studies. Nucleic Acids Res. 43 (7) gkv007.
Saba, R., et al., 2014. MicroRNA-146a: a dominant, negative regulator of the innate immune response. Front. Immunol. 5.
Schaller, J.-P., et al., 2016. Evaluation of the Tobacco Heating System 2.2. Part 2: Chemical Composition, Genotoxicity, Cytotoxicity, and Physical Properties of the Aerosol. Regul. Toxicol. Pharmacol. 81 (S2), S27–S47.
Schaller, J.-P., et al., 2016. Evaluation of the Tobacco Heating System 2.2. Part 3: Influence of the Tobacco Blend on the Formation of Harmful and Potentially Harmful Constituents in the Aerosol. Regul. Toxicol. Pharmacol. 81 (S2), S48–S58.

Schembri, F., et al., 2009. MicroRNAs as modulators of smoking-induced gene expression changes in human airway epithelium. Proc. Natl. Acad. Sci. 106, 2319–2324.
Sewer, A., et al., 2014. Assessment of a novel multi-array normalization method based on spike-in control probes suitable for microRNA datasets with global decreases in expression. BMC Res. notes 7, 302.
Sewer, A., et al., 2016. Evaluation of the Tobacco Heating System 2.2. Part 5: MicroRNA Expression from a 90-day Rat Inhalation Study Indicates Reduced Effects of the Aerosol on Lung Tissue Compared with Cigarette Smoke Exposure. Regul. Toxicol. Pharmacol. 81 (S2), S82–S92.
Shaykhiev, R., et al., 2009. Smoking-dependent reprogramming of alveolar macrophage polarization: implication for pathogenesis of chronic obstructive pulmonary disease. J. Immunol. 183, 2867–2883.
Smith, M., et al., 2016. Evaluation of the Tobacco Heating System 2.2. Part 1: Description of the System and the Scientific Assessment Program. Regul. Toxicol. Pharmacol. 81 (S2), S17–S26.
Suzuki, H.I., Miyazono, K., 2010. Dynamics of microRNA biogenesis: crosstalk between p53 network and microRNA processing pathway. J. Mol. Med. 88, 1085–1094.
Suzuki, H.I., et al., 2009. Modulation of microRNA processing by p53. Nature 460, 529–533.
Taganov, K.D., et al., 2006. NF-κB-dependent induction of microRNA miR-146, an inhibitor targeted to signaling proteins of innate immune responses. Proc. Natl. Acad. Sci. 103, 12481–12486.
Titz, B., et al., 2015. Alterations in the sputum proteome and transcriptome in smokers and early-stage COPD subjects. J. proteom. 128, 306–320.
Vaporidi, K., et al., 2012. Pulmonary microRNA profiling in a mouse model of ventilator-induced lung injury. Am. J. Physiol. Lung Cell. Mol. Physiol. 303, L199–L207.
Vrijens, K., et al., 2015. MicroRNAs as potential signatures of environmental exposure or effect: a systematic review. Environ. health Perspect. 123, 399.
Westra, J.W., et al., 2013. A modular cell-type focused inflammatory process network model for non-diseased pulmonary tissue. Bioinforma. Biol. Insights 7, 167.
Wiesen, J.L., Tomasi, T.B., 2009. Dicer is regulated by cellular stresses and interferons. Mol. Immunol. 46, 1222–1228.
Wong, E.T., et al., 2016. Evaluation of the Tobacco Heating System 2.2. Part 4: 90-day OECD 413 Rat Inhalation Study with Systems Toxicology Endpoints Demonstrates Reduced Exposure Effects Compared with Cigarette Smoke. Regul. Toxicol. Pharmacol. 81 (S2), S59–S81.
Wu, D., et al., 2013. The use of miRNA microarrays for the analysis of cancer samples with global miRNA decrease. RNA 19, 876–888.
Ying, H., et al., 2015. MiR-127 modulates macrophage polarization and promotes lung inflammation and injury by activating the JNK pathway. J. Immunol. 194, 1239–1251.
Zanetti, F., et al., 2016. Systems toxicology assessment of the biological impact of a candidate Modified Risk Tobacco Product on human organotypic oral epithelial cultures. Chem. Res. Toxicol. 29, 1252–1269.
Zhang, W., et al., 2015. Autocrine/Paracrine human growth hormone-stimulated MicroRNA 96-182-183 cluster promotes epithelial-mesenchymal transition and invasion in breast Cancer. J. Biol. Chem. 290, 13812–13829.
Zhang, Y., et al., 2013. Expression profiles of miRNAs in polarized macrophages. Int. J. Mol. Med. 31, 797–802.